Società Italiana di Fisica
Italian Physical Society

XCVIII CONGRESSO NAZIONALE
Napoli 17 - 21 Settembre 2012

AMPEROMETRIC DETECTION OF QUANTAL CATECHOLAMINE SECRETION FROM INDIVIDUAL CELLS BY AN ION BEAM MICROFABRICATED SINGLE CRYSTALLINE DIAMOND BIOSENSOR

Federico Picollo

University of Torino
Physics Department

NIS Centre of Excellence

CNISM sez. Torino

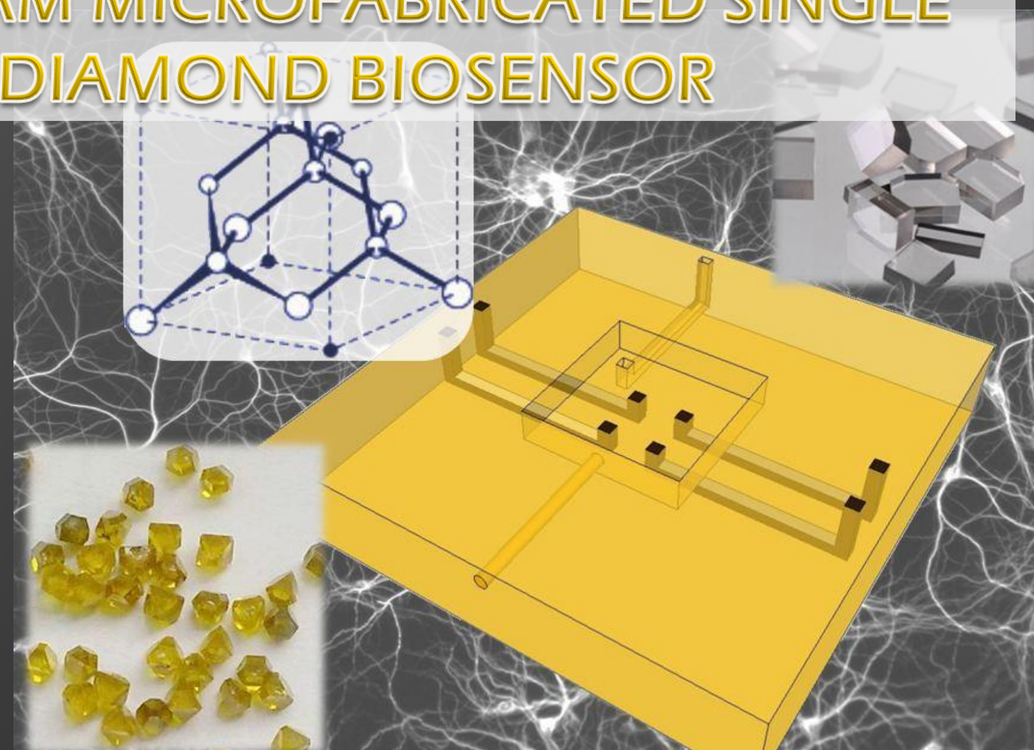

picollo@to.infn.it

Outline

- Introduction
  - *motivations of diamond micro-fabrication*
  - *interaction ion-diamond*

- Conductive channels fabrication
  - *sample masking*
  - *implantation*

- Channels characterization
  - *structural & electrical*
  - *thermal treatment dependence*

- Introduction^2
  - *chromaffin cells: what & why?*

- Prototype of biosensor
  - *exocytose measurement*

- Conclusions

INTRODUCTION

BIOSENSOR

A diamond-based cellular bio-sensor

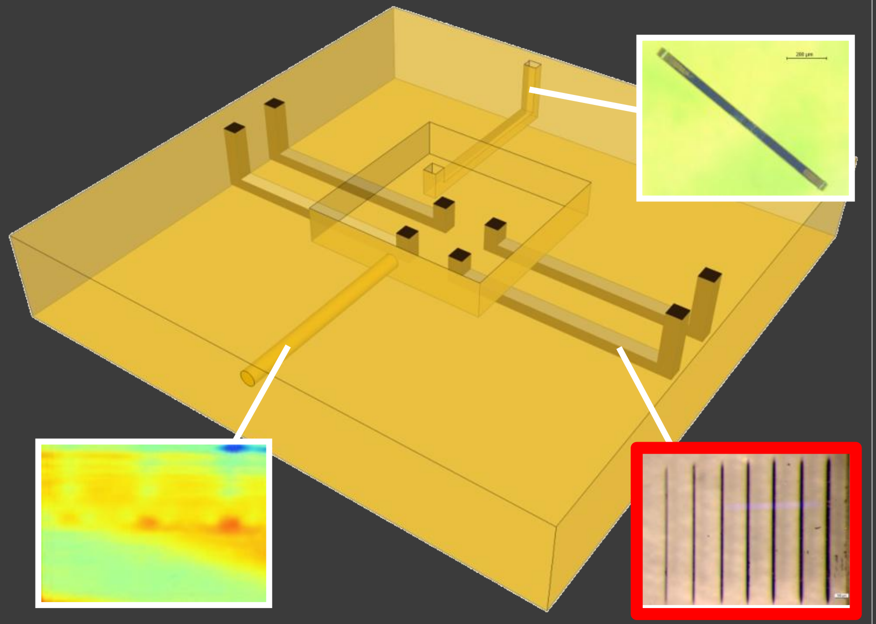

A bio-compatible and transparent diamond active substrate for interfacing with single excitable cells:

- electrical interfacing: micro-electrodes for cell sensing and stimulation
- optical interfacing: integrated waveguides
- chemical interfacing: microfluidic devices

Action potential

- important physiological process governing the presynaptic neurotransmitter release
- fast (~1-100 ms) membrane depolarization (-60 ÷ +50 mV) due to the entering of Na and Ca ions into an excitable cell
- voltammetric detection through capacitive coupling with micro-electrode arrays (MEAs)
- state of the art: issues with the chemical inertness of common substrates and with optical access for multi-parametric acquisition

Exocytosis

- secretion of catecholamines (adrenaline, noradrenaline) from vesicles in which they are highly concentrated
- state of the art: limited spatial resolution with conventional carbon fibers

Optical interfacing

- probing Ca concentration with specific fluorescent markers (Fura)
- state of the art: optical systems are not integrated in current MEAs

Chemical stimulation

- stimulation of specific receptors (i.e. nicotinic receptors)
- state of the art: limited use of microfluidic systems to perfuse chemicals and pharmaceuticals with high spatial resolution

Damage effect in diamond

at STP condition **diamond** is a **metastable** phase of carbon

graphite is a very different material with respect to diamond:

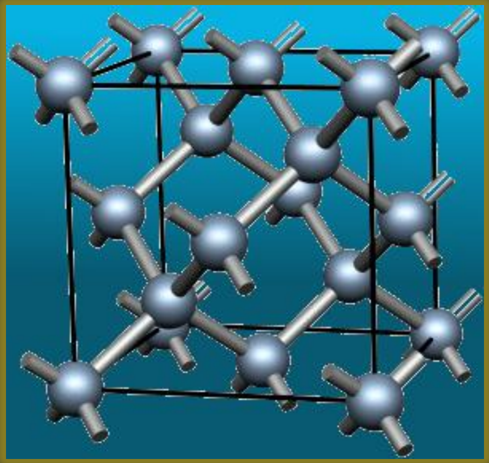

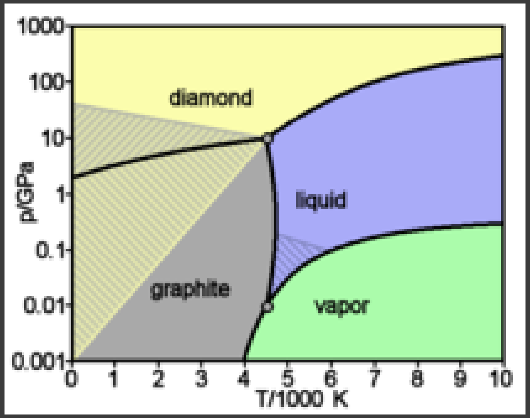

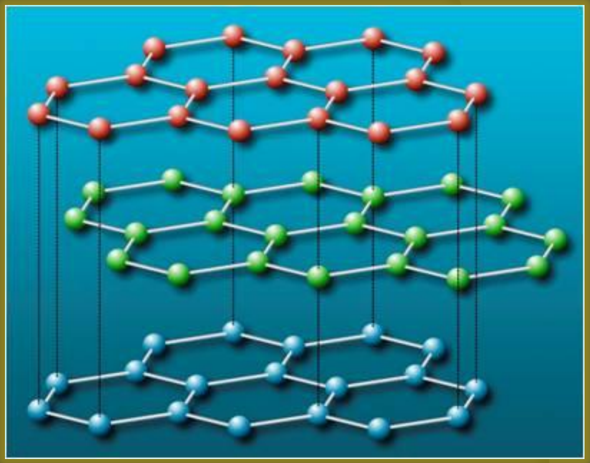

the **stable** one is the **graphite**
spontaneous conversion doesn't occur

it is soft, electrically conductive and **less chemically inert**

Damage effect in diamond

at STP condition **diamond** is a **metastable** phase of carbon

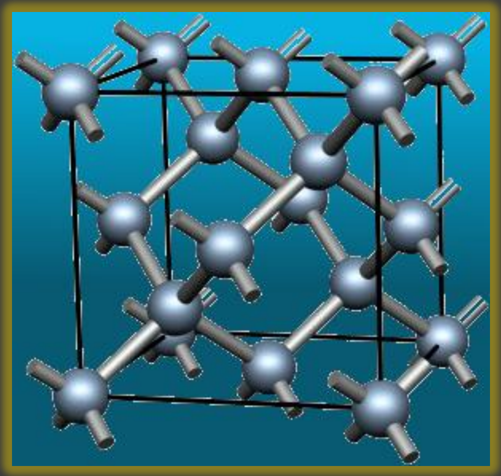

the **stable** one is the **graphite**

spontaneous conversion doesn't occur

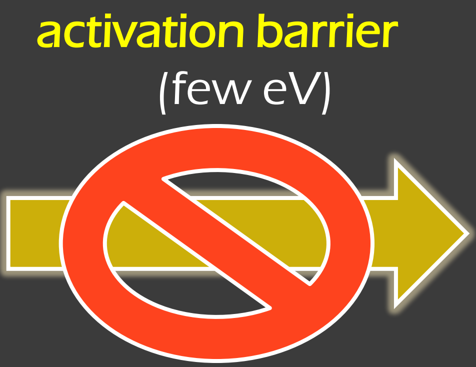

graphite is a <u>very different</u> material with respect to diamond:

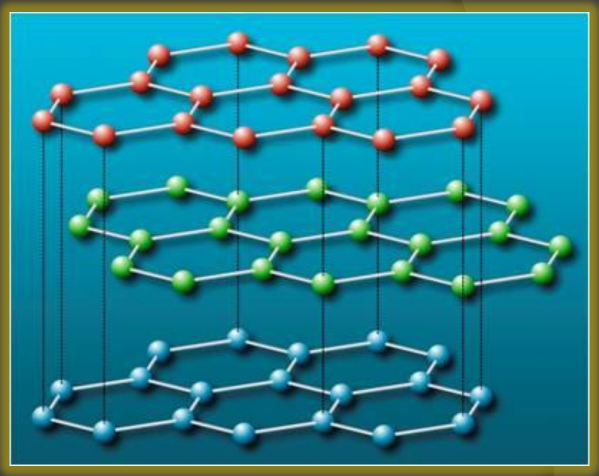

it is soft, <u>**electrically conductive**</u> and **less chemically inert**

Damage effect in diamond

at STP condition **diamond** is a **metastable** phase of carbon

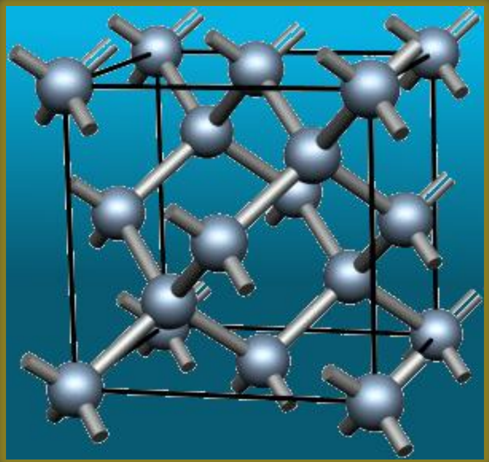

the **stable** one is the ***graphite***
spontaneous conversion doesn't occur

activation barrier
(few eV)

graphite is a <u>very different</u> material with respect to diamond:

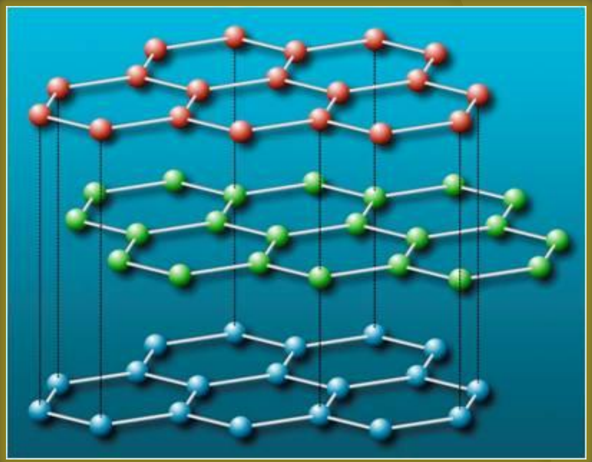

it is soft, <u>electrically conductive</u> and **less chemically inert**

External interaction

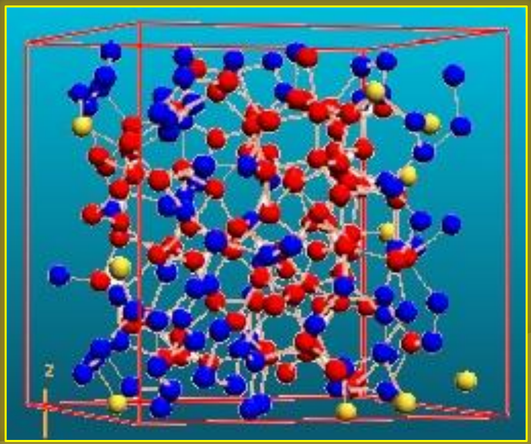

Thermal annealing

if the diamond lattice gets damaged / distorted it converts to graphite upon thermal annealing

Damage effect in diamond

Interaction of MeV light ions with matter

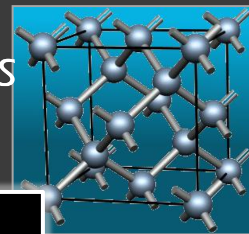

electronic energy losses

nuclear energy losses

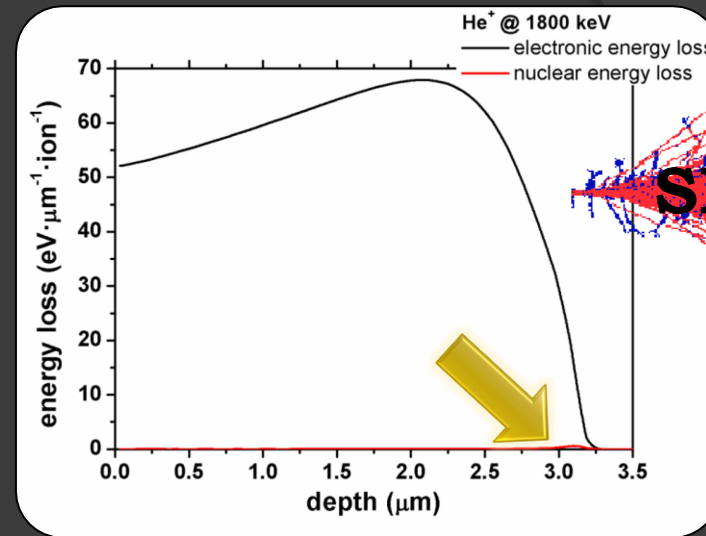

No remarkable structural effects associated with electronic energy losses

Damage effect in diamond

Interaction of MeV light ions with matter

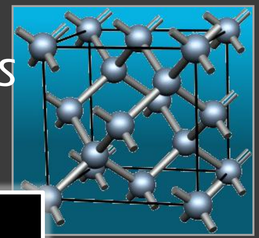

electronic energy losses

nuclear energy losses

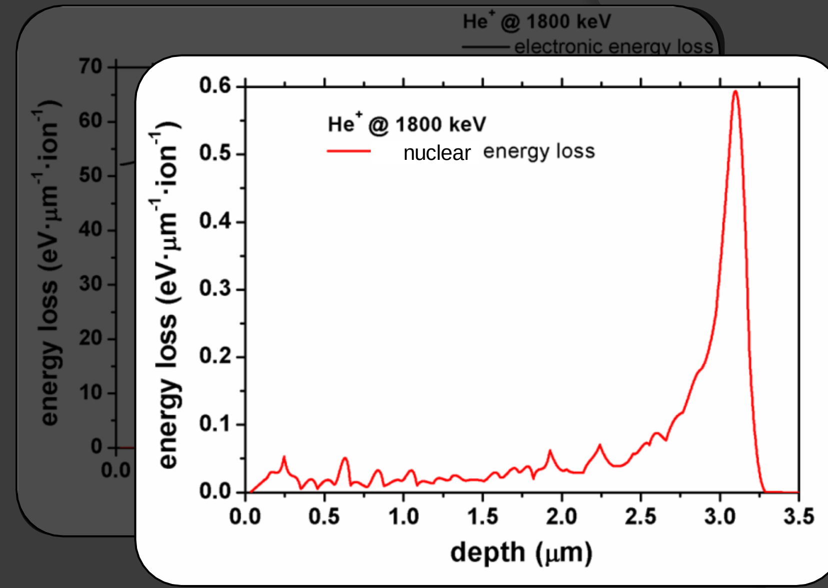

diamond conversion to amorphous carbon occurs at the end of range of ions

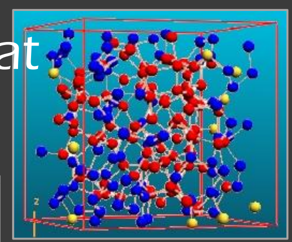

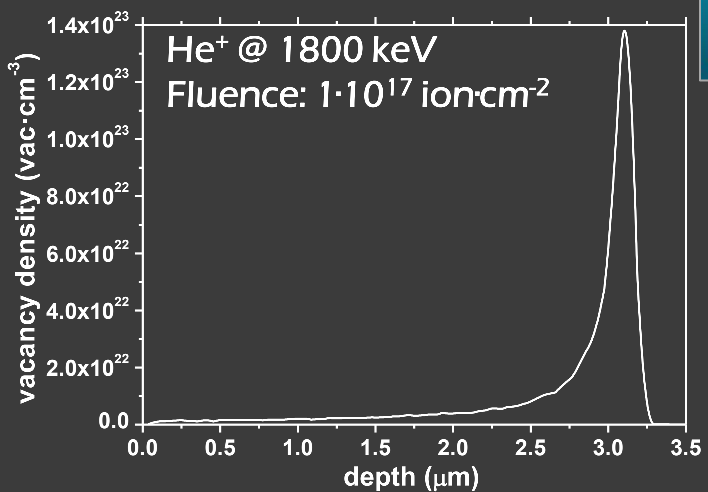

Damage effect in diamond

Interaction of MeV light ions with matter

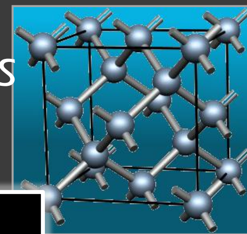

electronic energy losses

nuclear energy losses

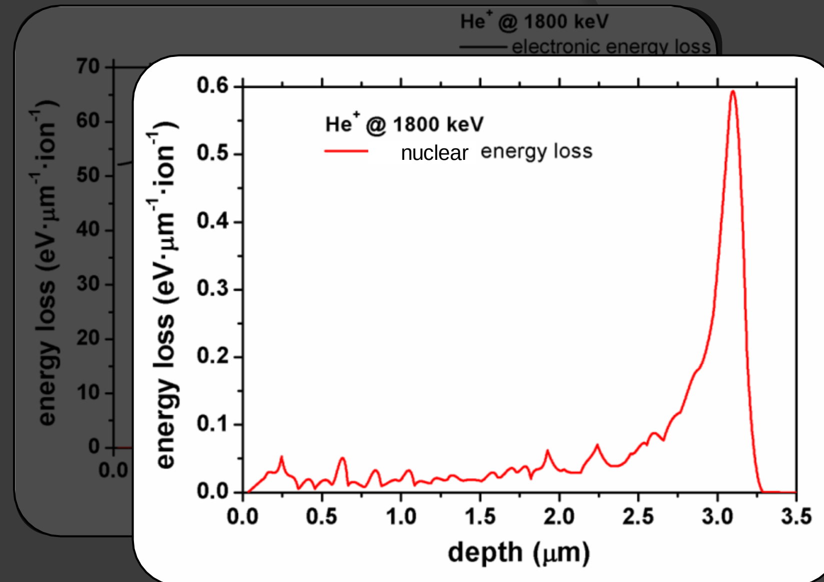

diamond conversion to amorphous carbon occurs at the end of range of ions

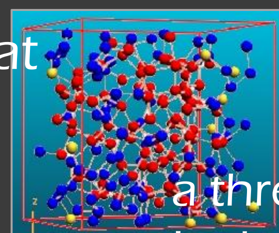

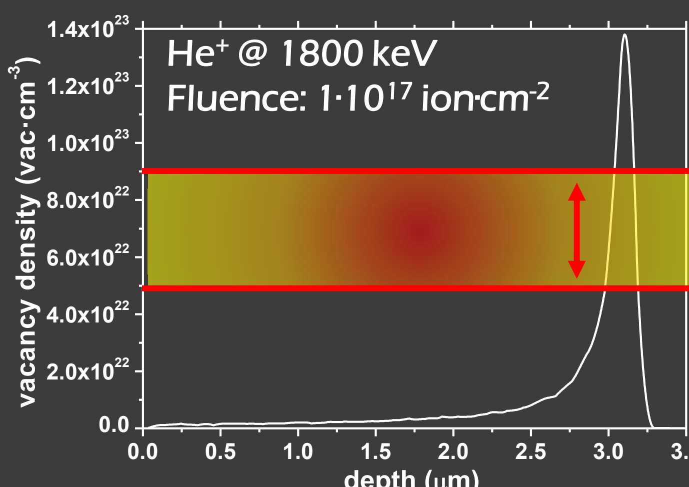

a threshold ("graphitization threshold") exists in the damage amount

if the vacancy density is

above the threshold, conversion to a graphitic-like phase occurs upon annealing

below the threshold the original structure is restored upon annealing

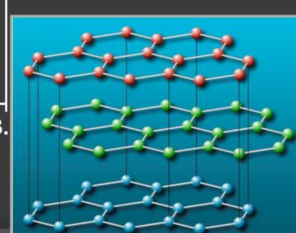

CONDUCTIVE CHANNELS FABRICATION

Ion direct writing on diamond

Synthetic Diamond

CVD

- ✓ homepitaxial single crystal
- ✓ [N] < 1 ppm, [B] < 0.05 ppm
- ✓ crystal orientation: {100}
- ✓ dimensions: 3×3 ×0.5 mm³

HPHT

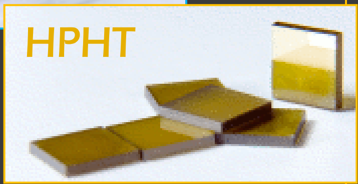

- ✓ High Pressure High Temperature single crystal
- ✓ [N] < 10 - 100 ppm,
- ✓ crystal orientation: {100}
- ✓ dimensions: 3×3 ×0.5 mm³

He⁺ @ 1800 keV

- ✓ raster scanning micro-beam (∅~10μm)
- ✓ ion current: ~ 3-10 nA

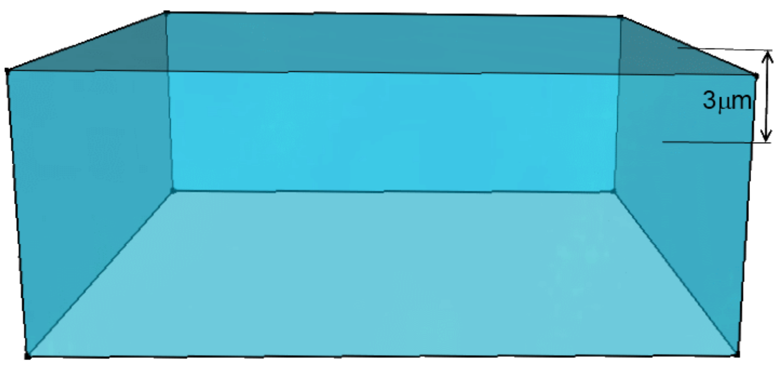

Implanted channels

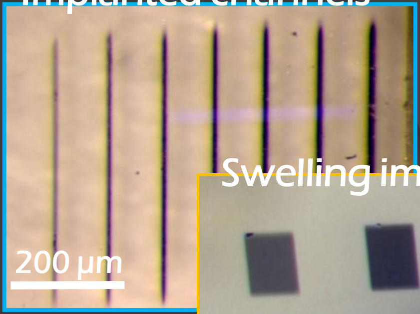

Swelling implantation

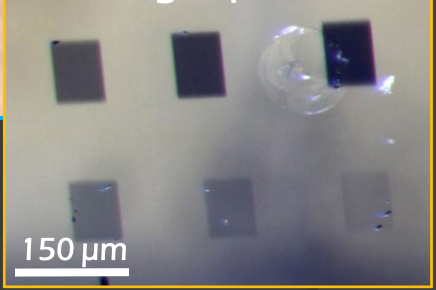

Ion direct writing on diamond

Synthetic Diamond

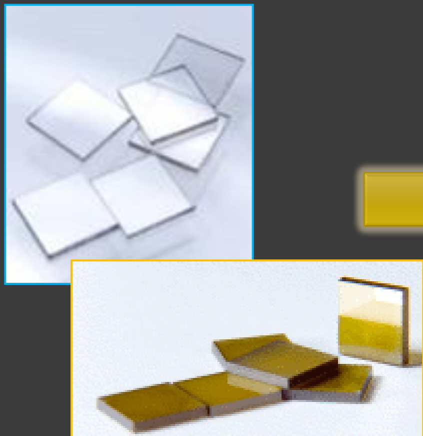

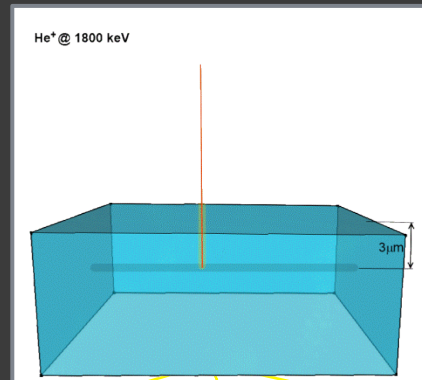

Implanted channels

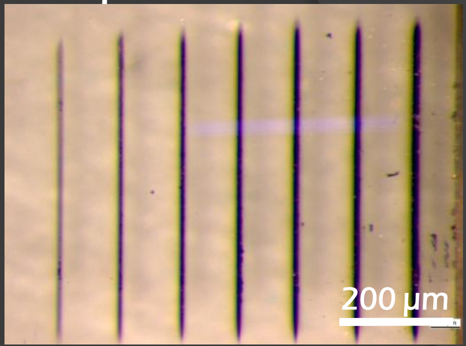

Implantation fluence

✓raster scanning micro-beam (∅ ~ 10 µm)
✓ion current: ~ 3-10 nA

Electrical characterization samples

Structural characterization samples

Laboratory for Ion Beam Interactions, Ruđer Bošković Institute – Zagreb (Croatia): C @ 6 MeV

C^{+++} @ 6000 keV
Fluence range:
$2 \cdot 10^{16}$ - $5 \cdot 10^{17}$ cm^{-2}

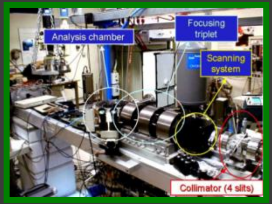

AN2000 accelerator, INFN National Laboratories of Legnaro – Padova (Italy)

He^+ @ 1300 - 1800 keV
Fluence range:
$3 \cdot 10^{16}$ - $5 \cdot 10^{17}$ cm^{-2}

MP2 beamline, MicroAnalytical Research Centre, University of Melbourne – Melbourne (Australia)

He^+ @ 500 keV
Fluence range:
$2 \cdot 10^{16}$ - $1 \cdot 10^{17}$ cm^{-2}

Variable thickness masking

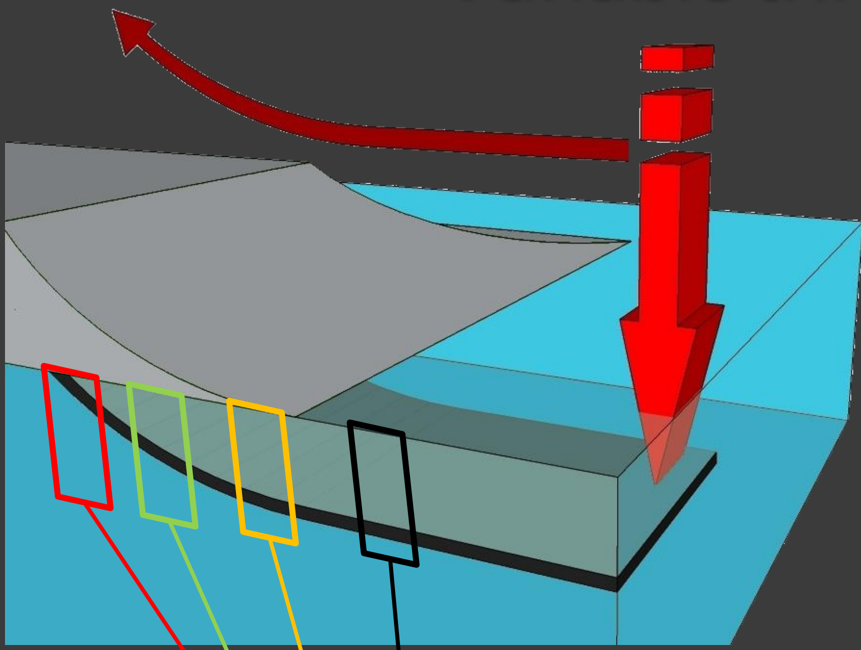

Control of ions penetration by means of a variable thickness mask*

ions lose energy passing through the mask

Shallower highly damaged layer

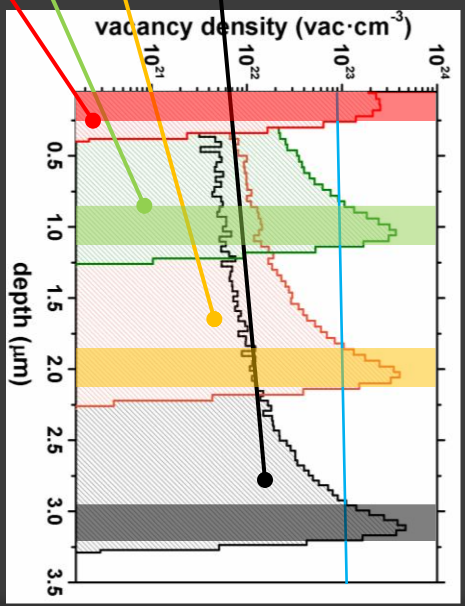

Thermal evaporation of silver through a patterned mask of an array of rectangular holes

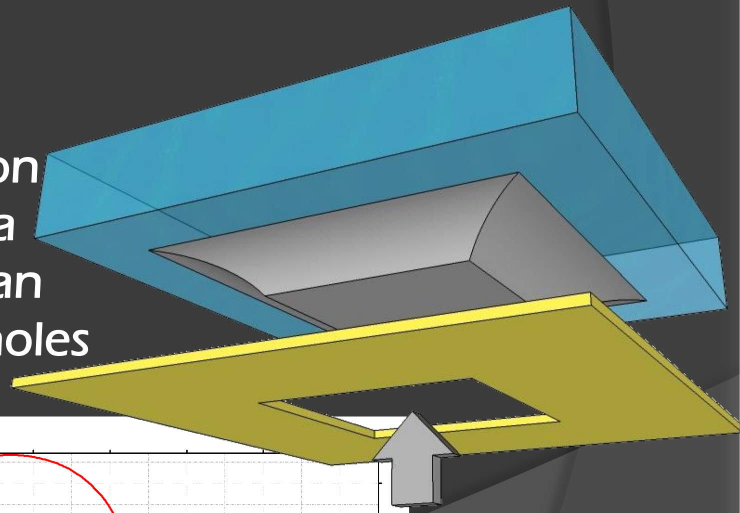

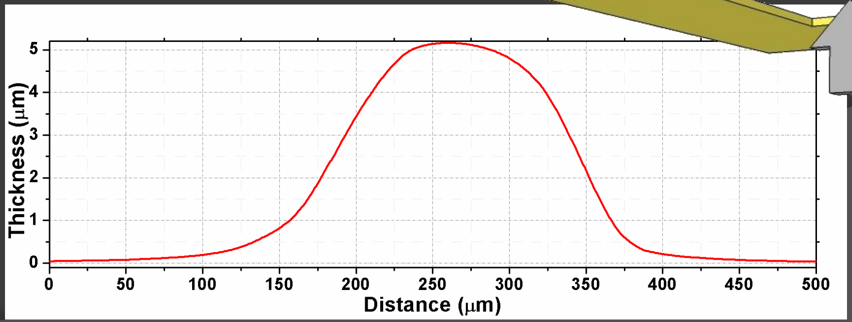

* P. Olivero et al., Diamond Relat. Mater. 18, 870 (2009)

CONDUCTIVE CHANNELS CHARACTERIZATION

TEM cross sections images

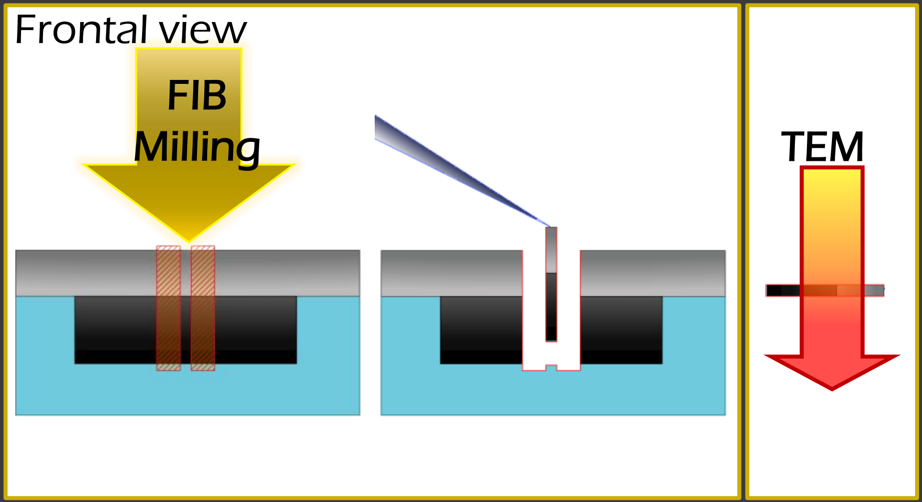

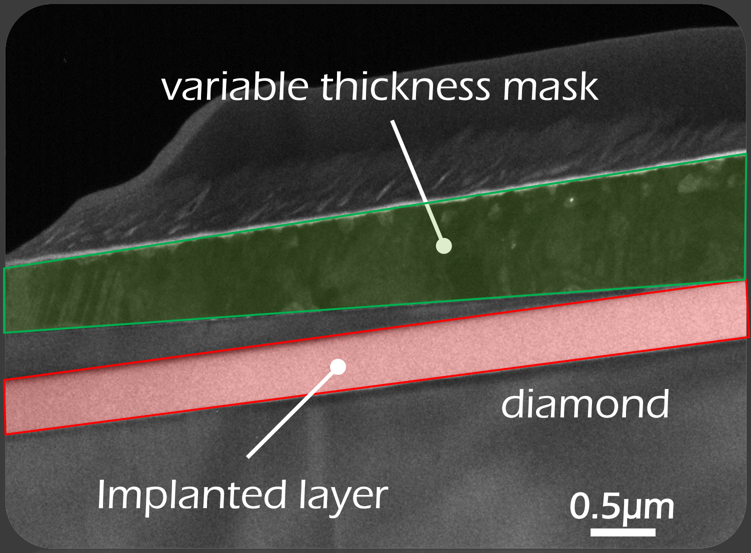

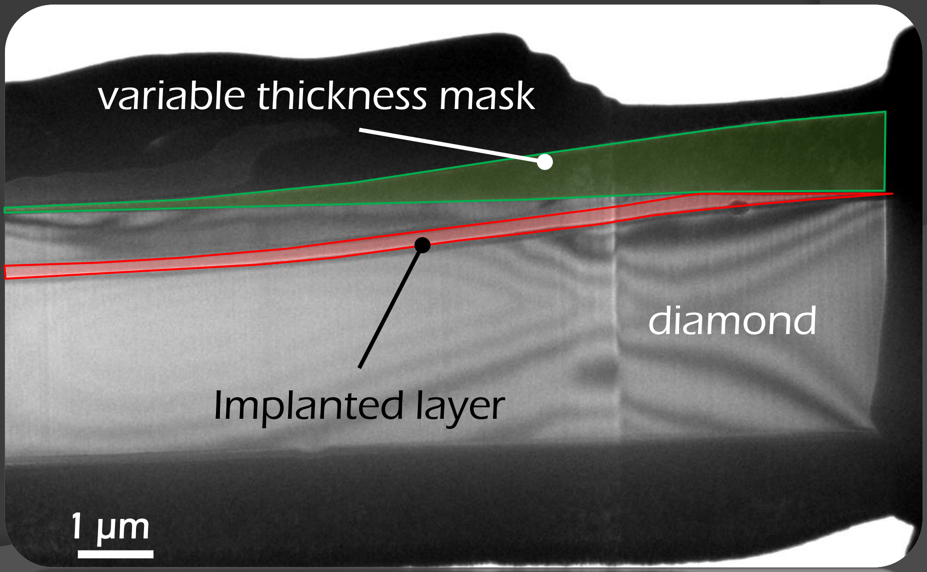

Electrical characterization: as-implanted sample

Implanted channels

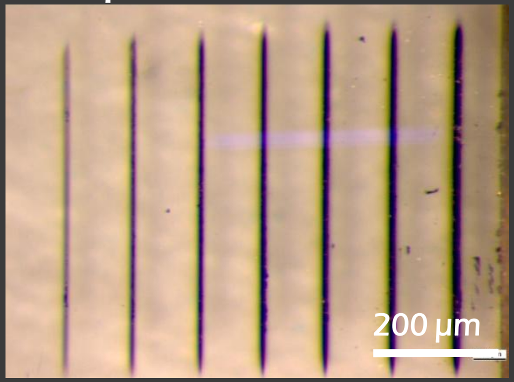

Implantation fluence

Channels length: 400 µm
width: 20 µm

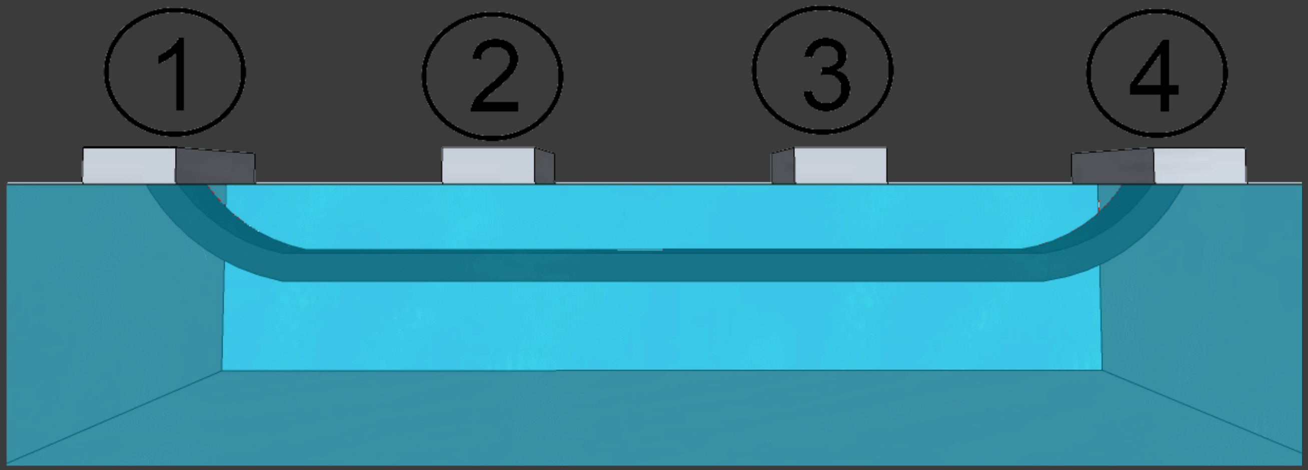

Electrical characterization: as-implanted sample

Implanted channels

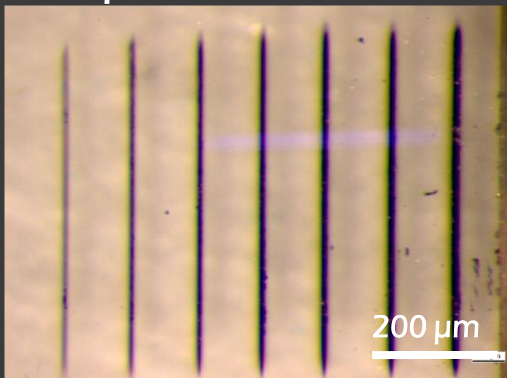

Implantation fluence

Channels length: 400 µm
width: 20 µm

Highly damaged layer

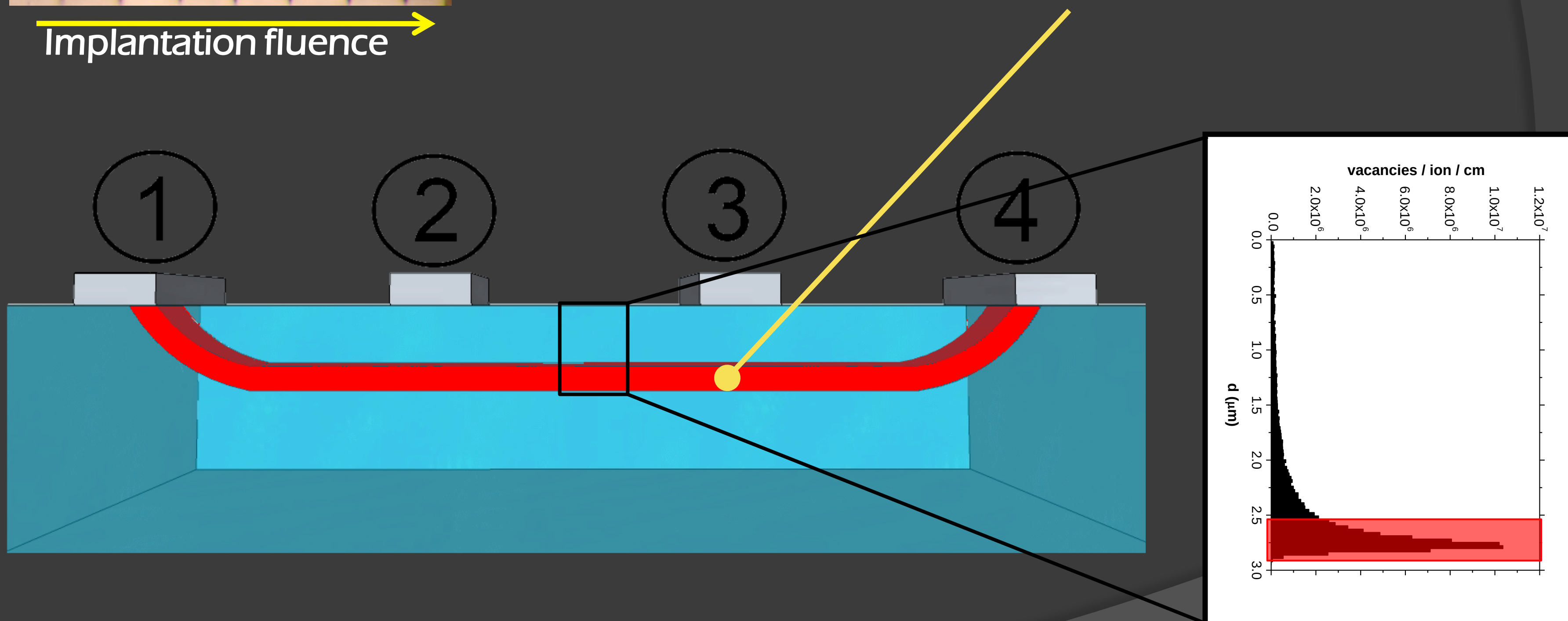

Electrical characterization: as-implanted sample

Implanted channels

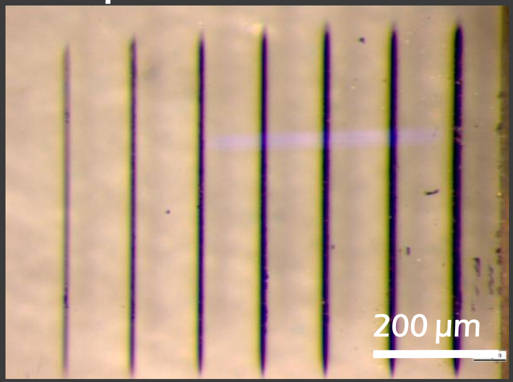

Implantation fluence

Channels length: 400 µm
width: 20 µm

Cap Layer

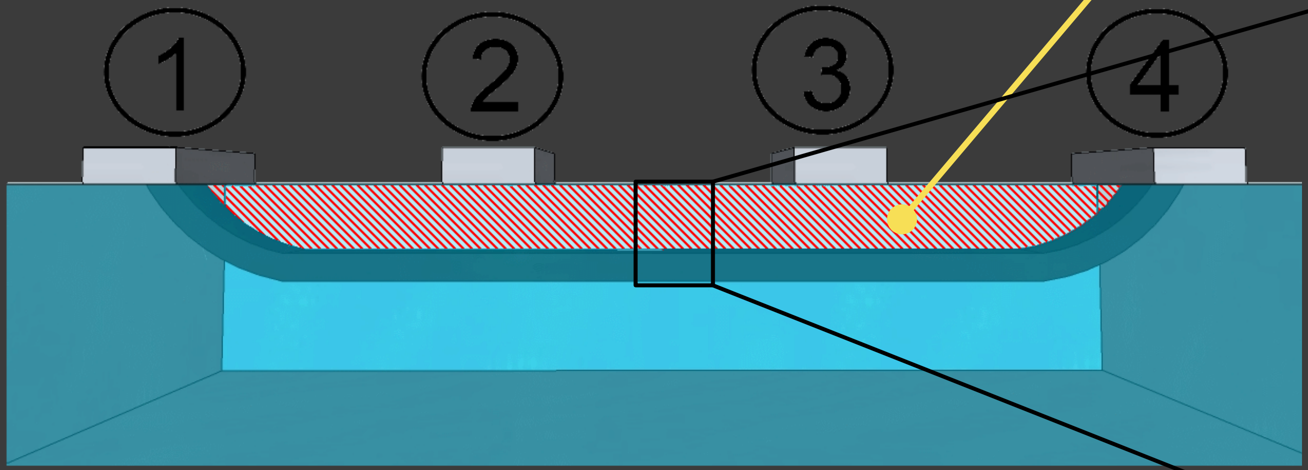

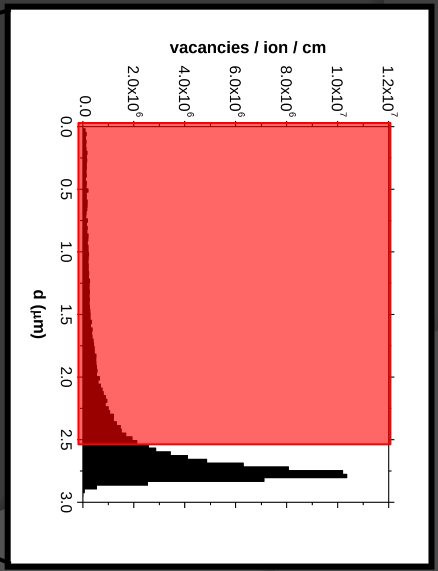

Electrical characterization: as-implanted sample

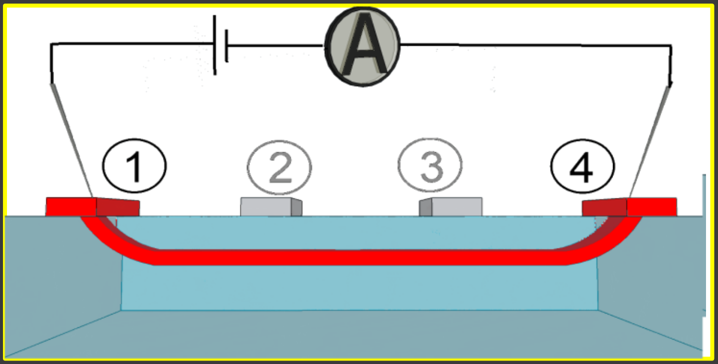

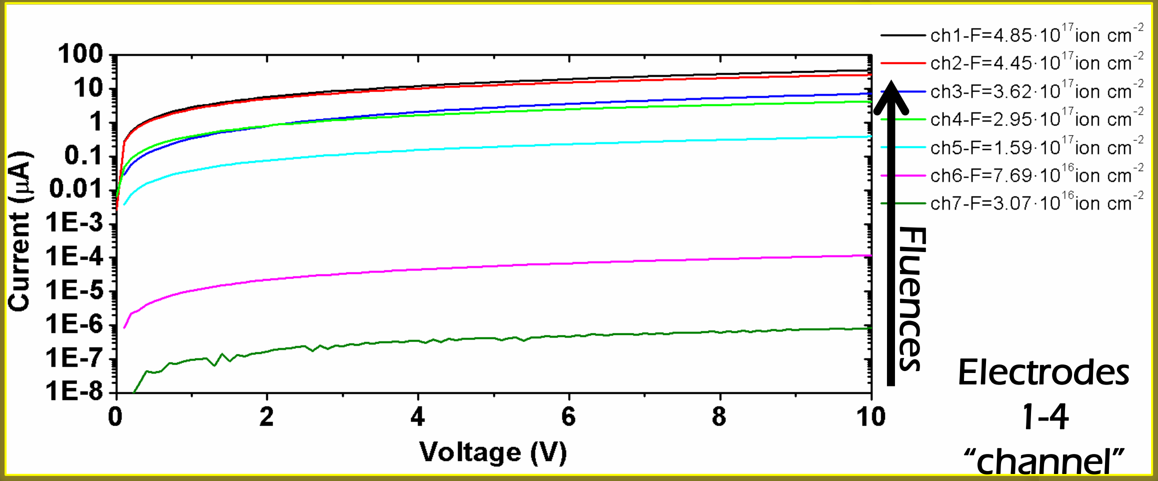

!! dependence between conductivity (G) and implantation fluence (F) → increasing F increase G

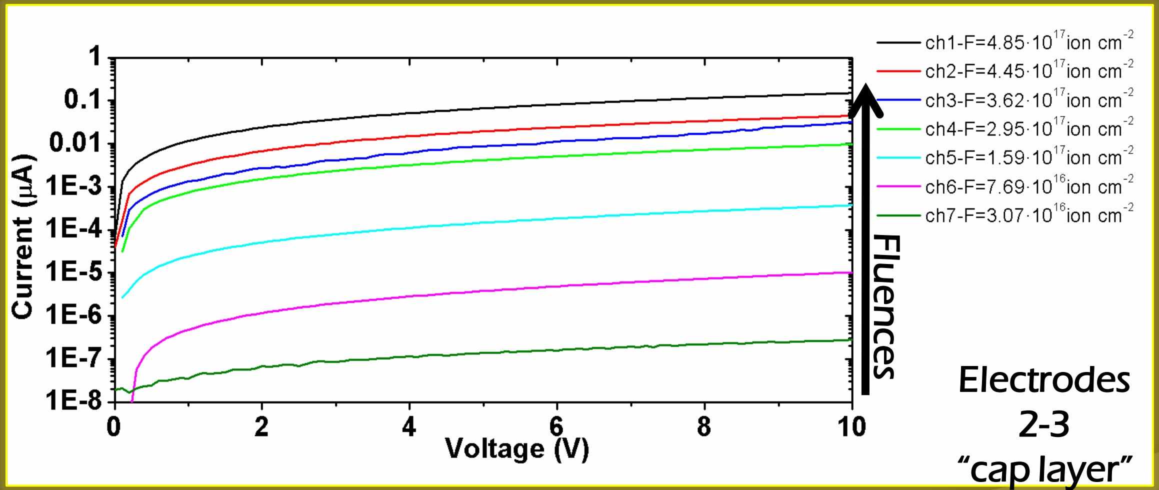

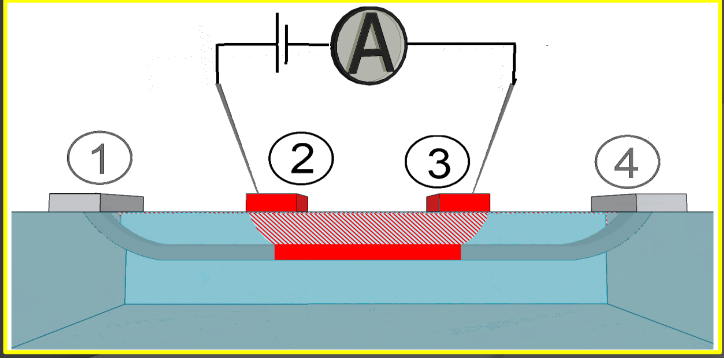

Electrical characterization: conduction mechanism

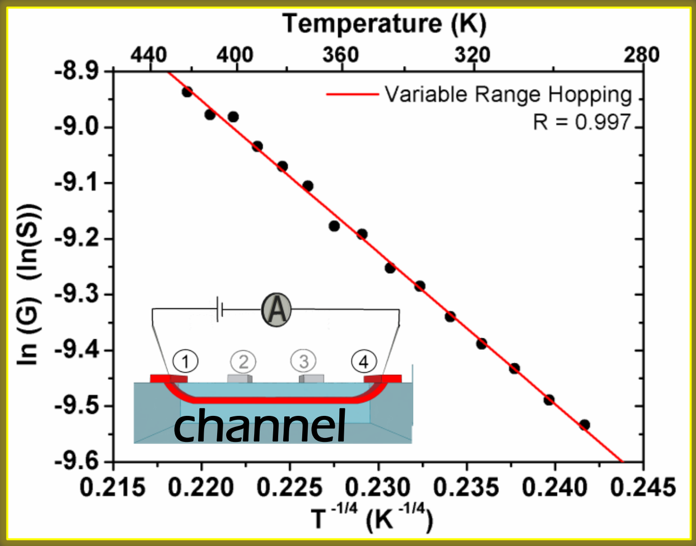

Sample 1 $N(E_F)=2.2\cdot 10^{20}\ eV^{-1}\cdot cm^{-3}$

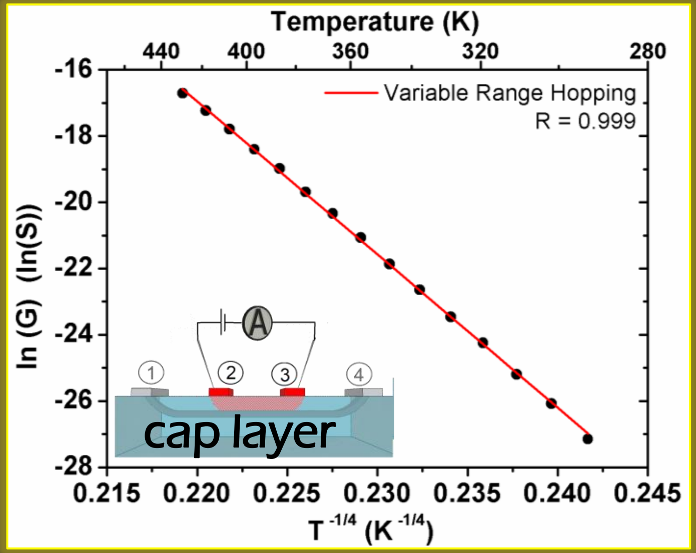

$N(E_F)=2.7\cdot 10^{15}\ eV^{-1}\cdot cm^{-3}$

Three-dimensional variable range hopping conductance*

$$G(T)=G_0(T)\cdot \exp\left[-\left(\frac{T_0}{T}\right)^{1/4}\right]=G_{00}\cdot T^{-1/2}\cdot \exp\left[-\left(\frac{T_0}{T}\right)^{1/4}\right]$$

$$T_0=\left(\frac{512}{9\pi}\right)\frac{\alpha^3}{k_B N(E_F)}$$

Mott 1960

G_{00} = temperature-independent pre-factor
$N(E_F)$ = density of trap states at the Fermi level
α = decay parameter of the localized wave function**

Typical for amorphous system

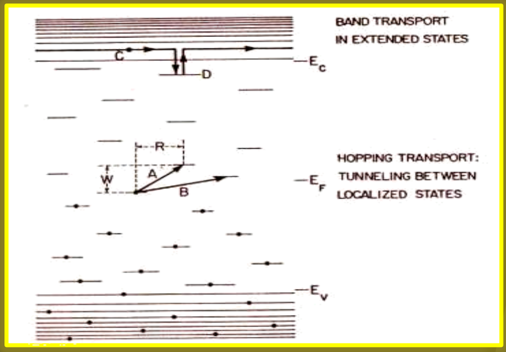

✓ Cap layer & channel conduce with the same conduction mechanism
✓ At all the fluences, G(T) follows the Variable Range Hopping model

* S. Prawer and R. Kalish, **Phys Rev. B 51**, 15711 (1995)
* F. Picollo et al., **Diam- Relat. Mater. 19**, 466 (2010)
** J.J. Hauser et al., **Appl. Phys. Lett. 30**, 129 (1976)

Thermal annealing effect

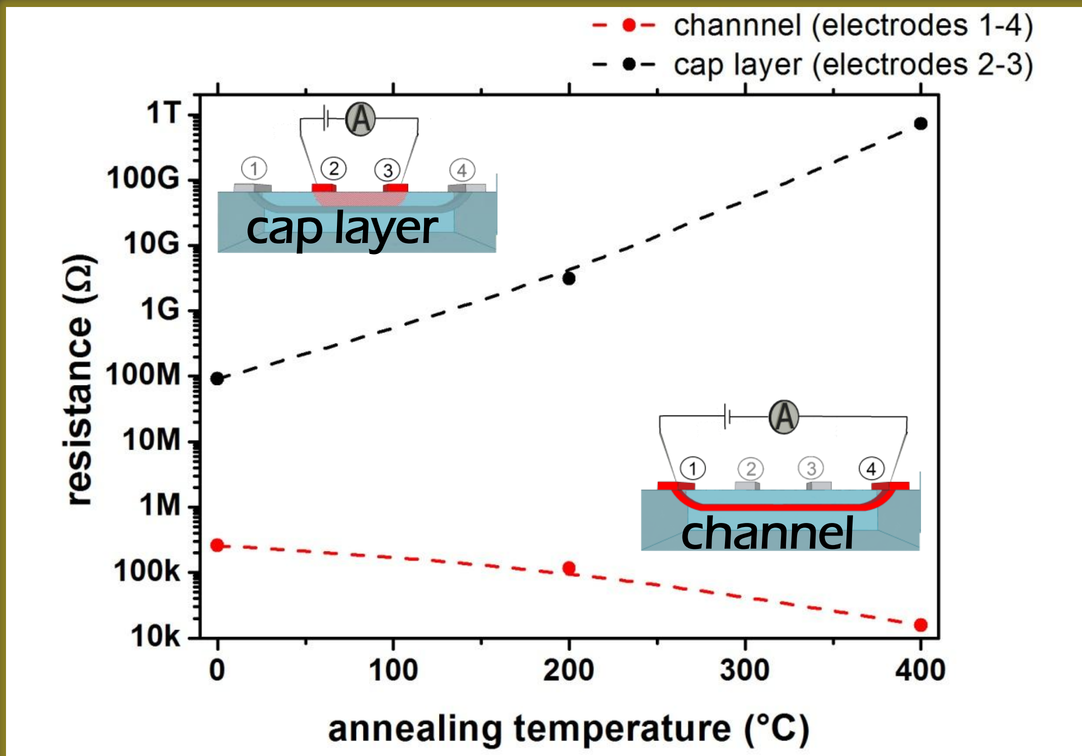

Thermal annealing

✓ the cap layer decrease its conductivity

✓The channel increase its conductivity

the conductive channels are surrounded by a insulating diamond matrix

Electrical characterization: conduction mechanism

Sample annealed @ 1000°C

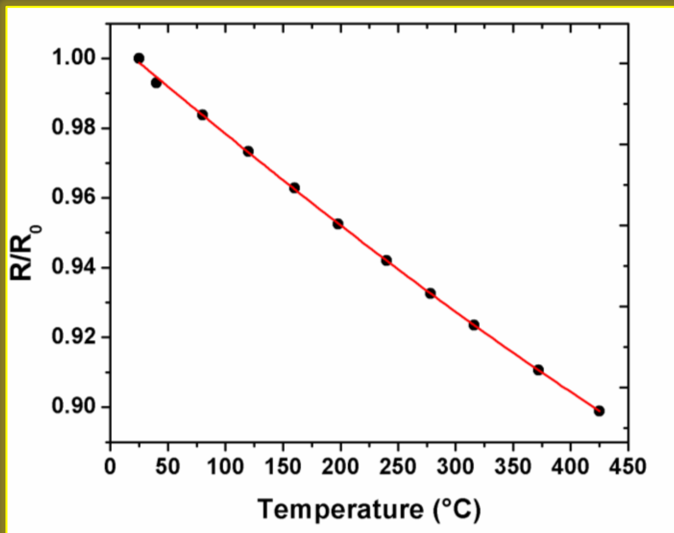

Sample 2

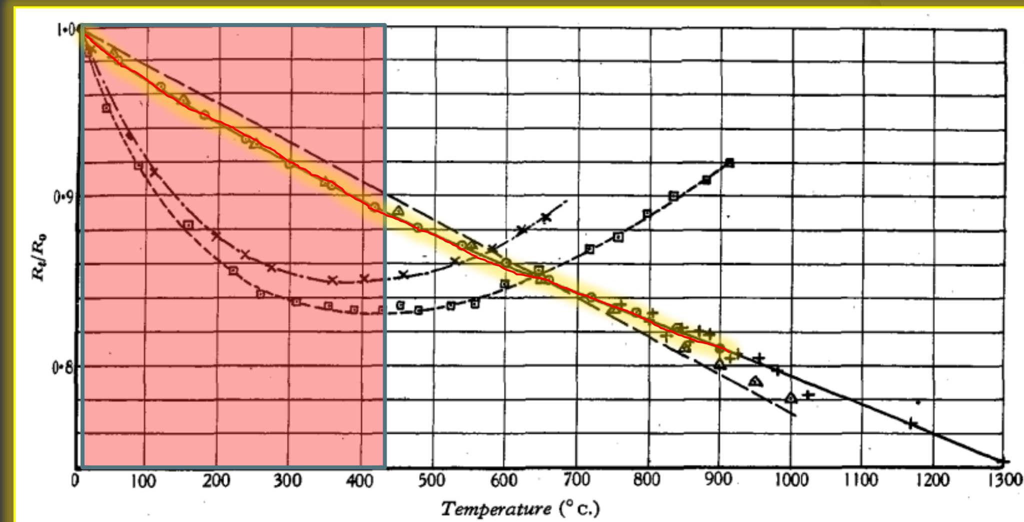

L. J. Collier et al.,
Proc. Phys. Soc. 51, 147 (1939)

✓ Channels implanted above graphitization threshold

✓ The conduction properties are compatible with those of carbon rod

graphite*
$\rho \approx 1.4 \cdot 10^{-3}\ \Omega \cdot cm$

diamond*
$\rho > 10^{14}\ \Omega \cdot cm$

channels
$\rho \approx 1.4 - 1.6 \cdot 10^{-3}\ \Omega \cdot cm$

$\rho_{diamond} / \rho_{channel} > 10^{17}$

* J. F. Prins et al.,
Phys. Rev. B 31, 2472 (1985)

PROTOTYPE OF CELLULAR EXOCYTOSE DETECTOR

Chromaffin cells: what are they?

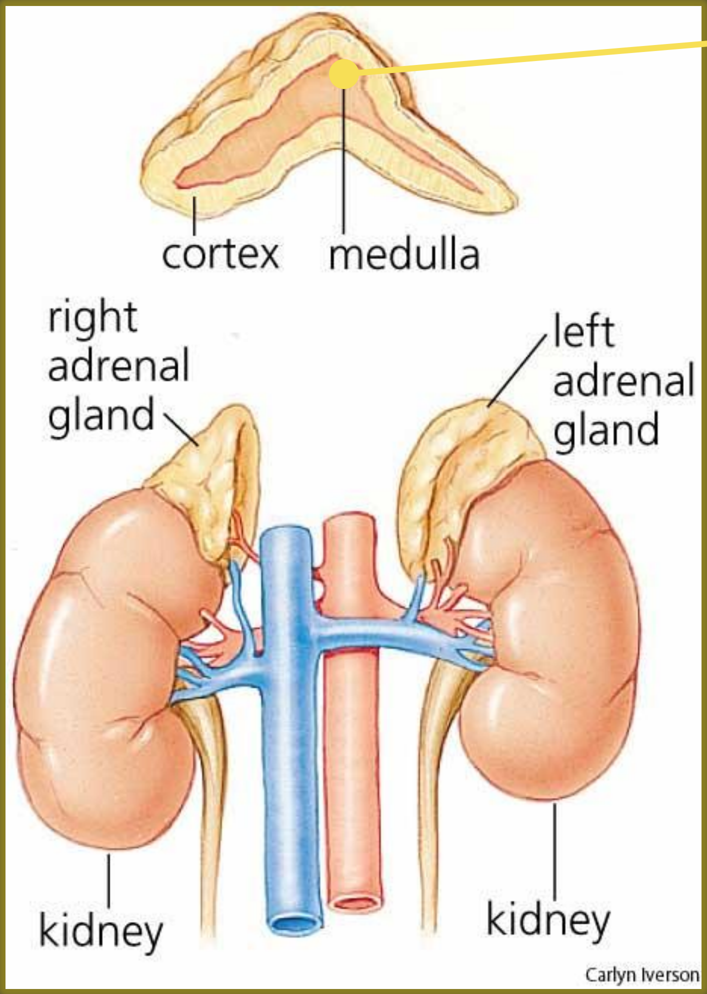

- ✓ located into the medulla part of adrenal gland
- ✓ releases **adrenaline** and **noradrenaline**

Chromaffin cells: what are they?

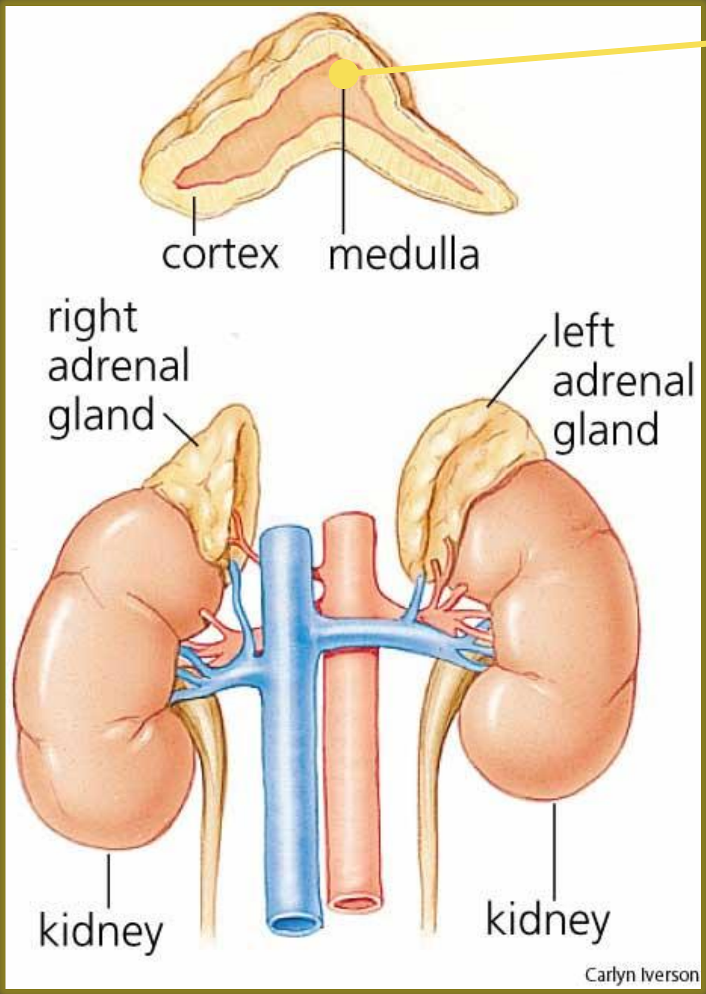

- ✓ located into the medulla part of adrenal gland
- ✓ releases **adrenaline** and **noradrenaline**

governs the "fight or flight" response

Chromaffin cells: what are they?

✓ located into the medulla part of adrenal gland

✓releases **adrenaline** and **noradrenaline**

governs the “fight or flight" response

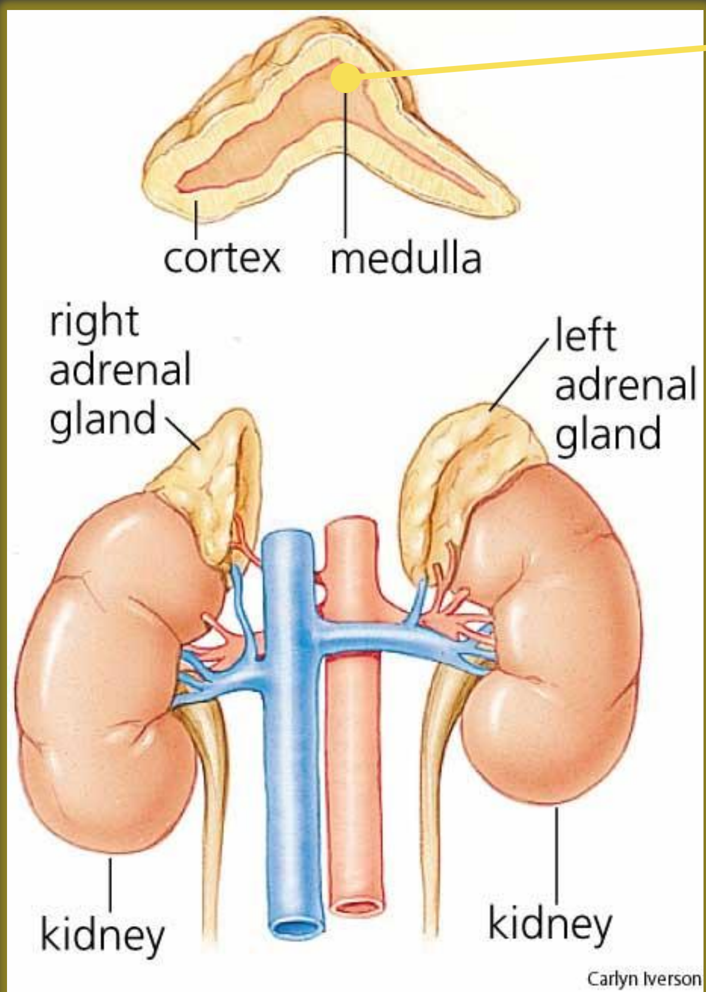

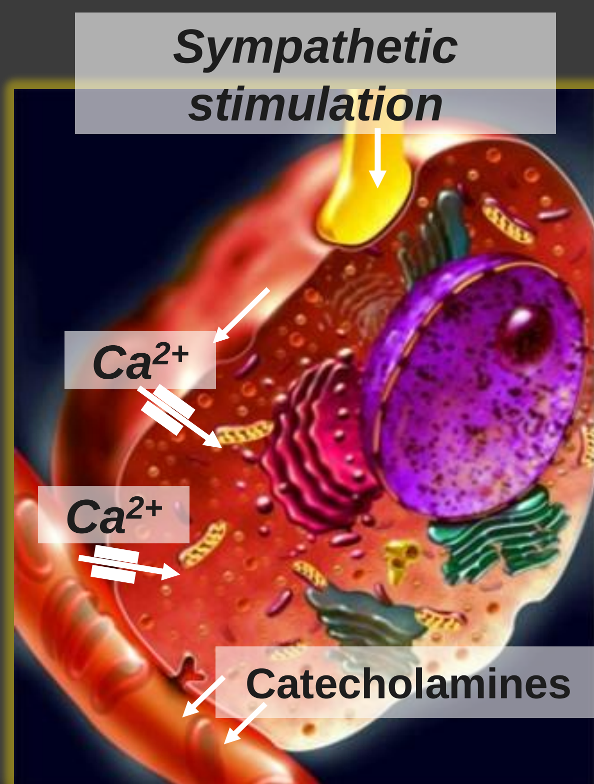

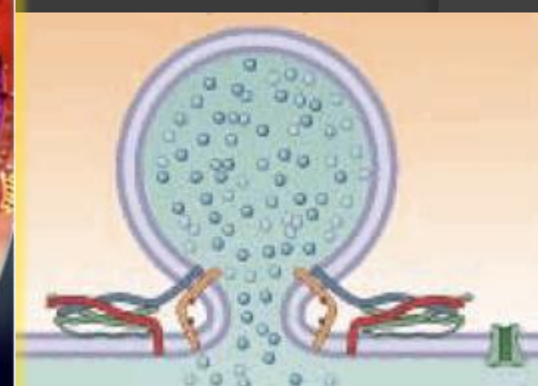

Chromaffin cells: model for the study of secretion

- ✓ **Model of neurons excitation-secretion**
- ✓ Easily available → large dimensions (>10 μm)
- ✓ Voltage-gated Ca^{2+} channels
- ✓ Electrically excitable
- ✓ Containing chromaffin granules
  - ✓ Diameter = 50 ÷ 300 nm
  - ✓ Catecholamines

    Concentration = 0.5 - 1 M

    (~10^6 molecules each granule)

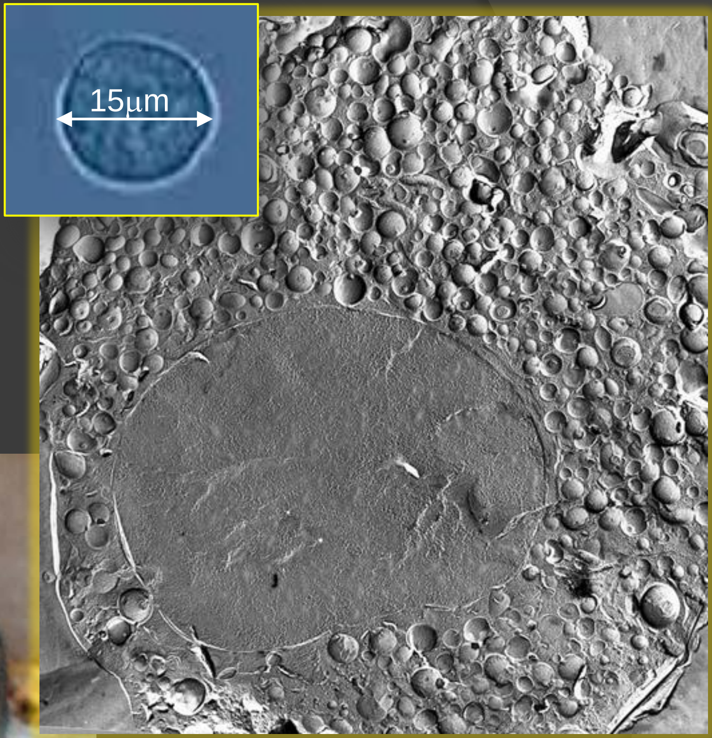

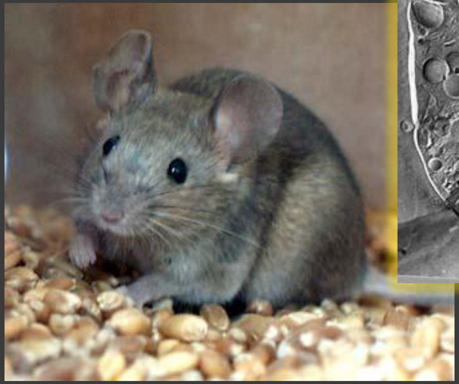

Catecholamines

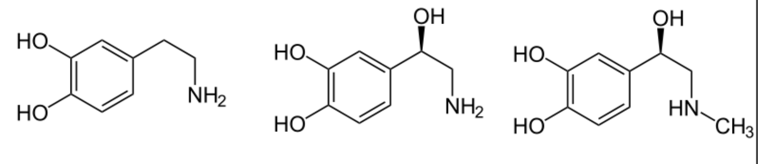

dopamine noradrenaline adrenaline

Chromaffin cells: model for the study of secretion

Exocytose process related to synaptic transmission interesting for

- physiology → neurodegenerative disease
- pharmaceutics →
  - antidepressants
  - anxiolytics
  - drugs treat Parkinson
  - drugs treat Alzheimer

Measurements of secretion

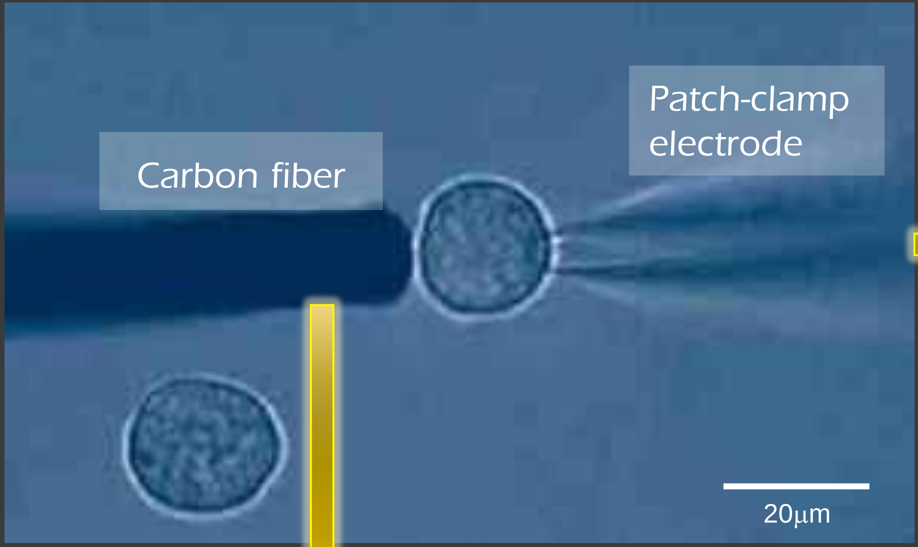

Capacitance measurement (indirect measurement)

$$C \propto S$$

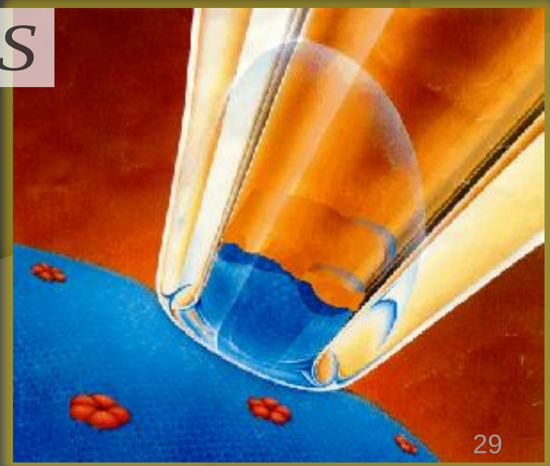

Amperometry (direct measurement)

Amperometry

Adrenaline oxidation

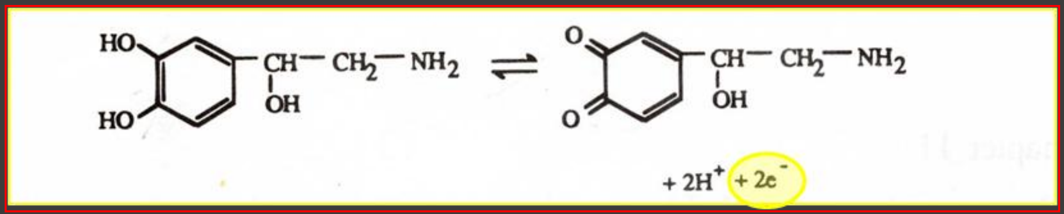

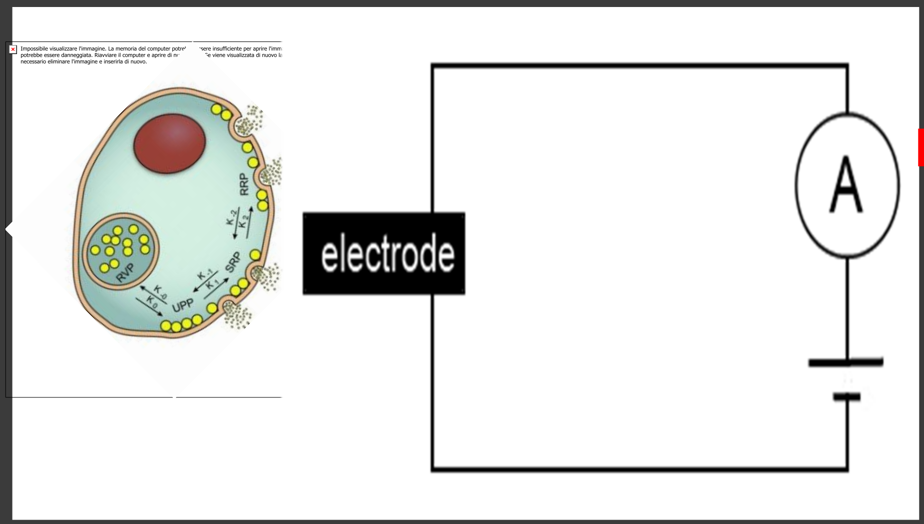

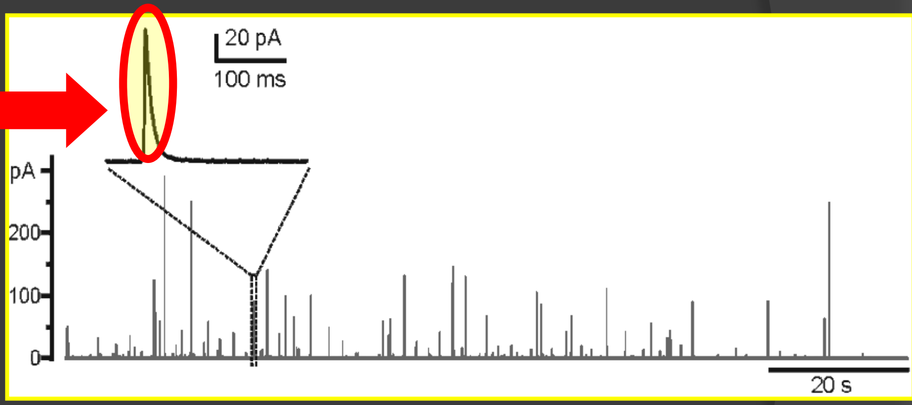

Current Spikes

- ✓Amplitude ~ 10-500 pA
- ✓Duration ~ 10-100 ms
- ✓Each spike is due to the fusion of one granule

Carbon micro-fiber vs. diamond biosensor - 1

Carbon fiber micro-electrode

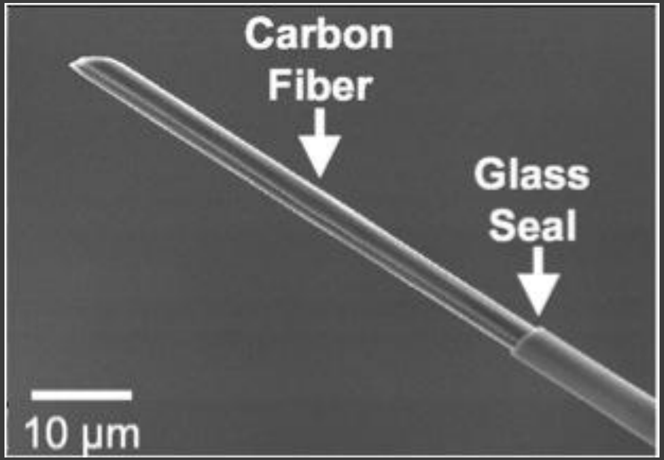

ADVANTAGES

✓high temporal resolution (<ms)

✓ high sensibility (pA)

✓ not invasive technique

✓Simple to implement

DRAWBACKS

✓Low spatial resolution (~ 30 μm^2)

✓ Limited use on single cell

Diamond based bio-sensor

KEY ADVANTAGES

✓bio-compatibility

✓chemical inertness

✓wide electrochemical window

✓Suitable to be functionalized

✓Optically transparent

REQUIREMENTS

Availability of a robust technique for diamond micromachining and to produce carbon-based conductive microelectrodes.

Prototype of biosensor

- diamond:
  - HPHT,
  - single crystal,
  - type Ib,
  - 3×3×1.5 mm^3
- He @ 1.6 MeV
- thermal annealing @ 1100 °C ×2 hours

- Channel dimensions:
  - 2 mm × 50 μm

Electrical characterization

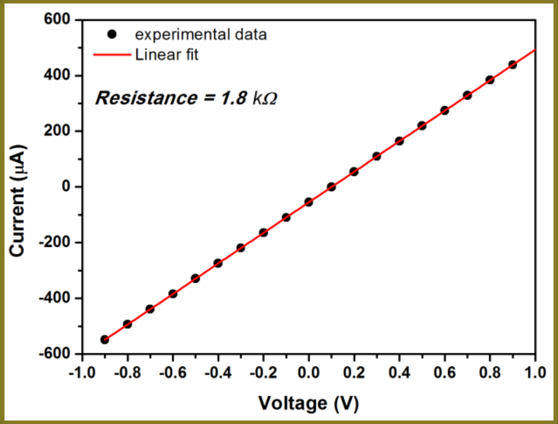

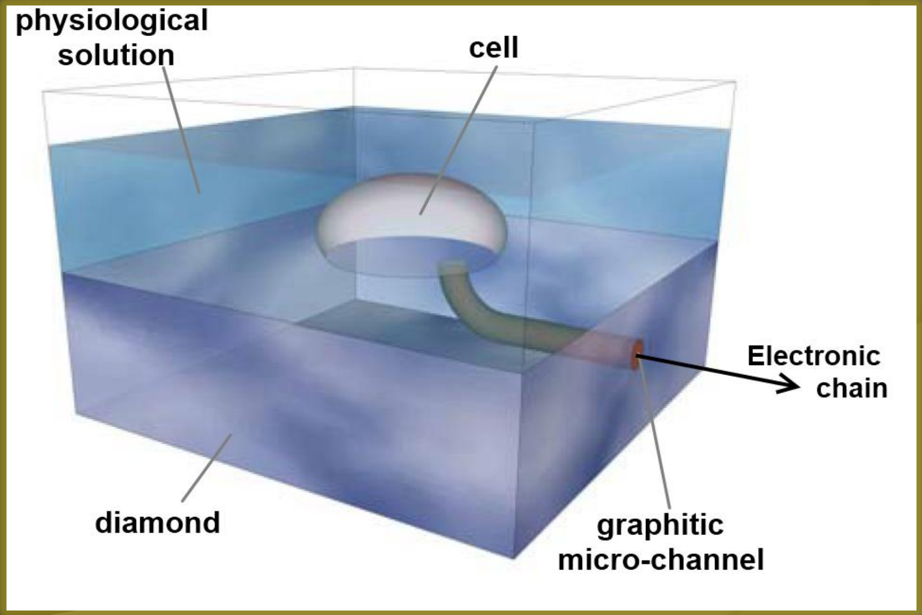

Adrenaline oxidation tests

Cyclic voltametry information:

- ✓ electrochemical window → > 1.5 V
- ✓ bias for oxidize adrenaline → >800 mV

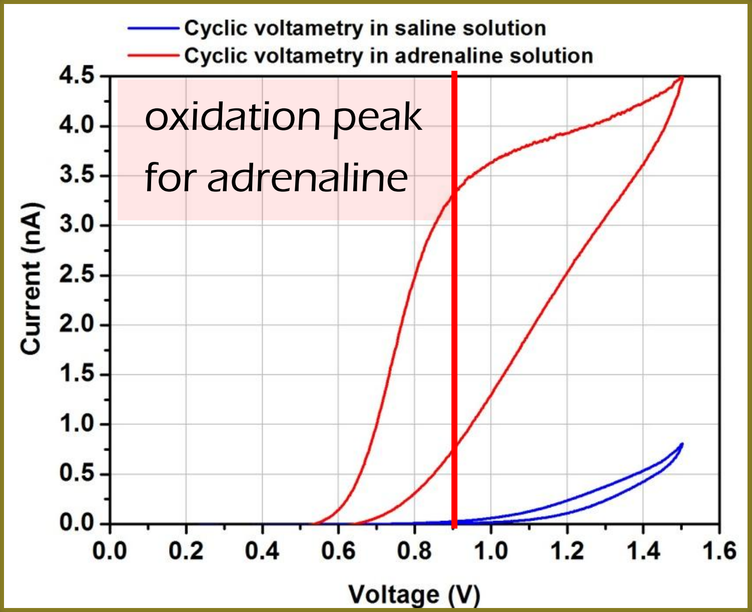

Potential run from 0 V to 1.5 V with 50 mV/s scan rate

Micro-perfusion:

- ✓ detection of low volume of adrenaline

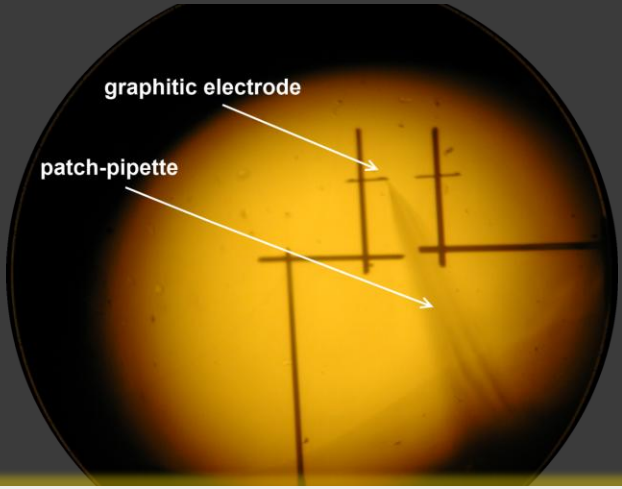

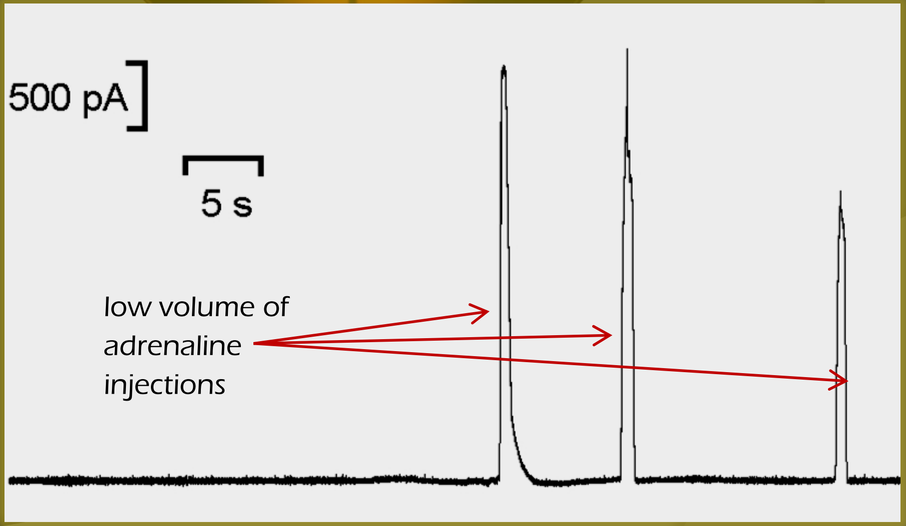

Detection of catecholamine

The cells were:
- Grown in suspension
- Centrifuged and placed in saline solution

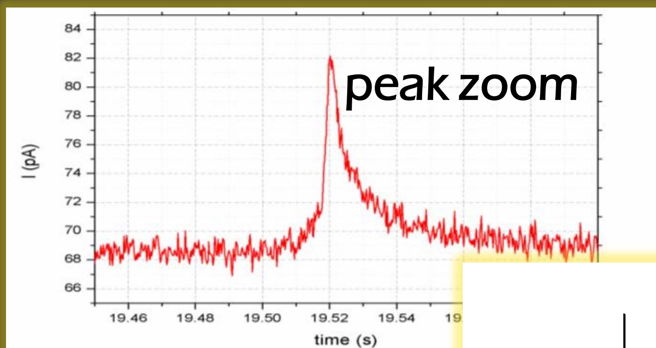

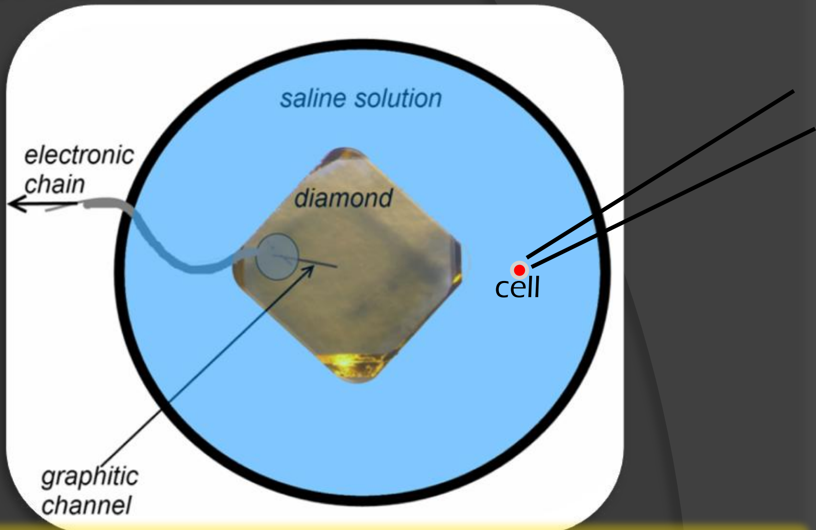

External stimulation:
KCl-enriched solution

Signal recording for 240 s

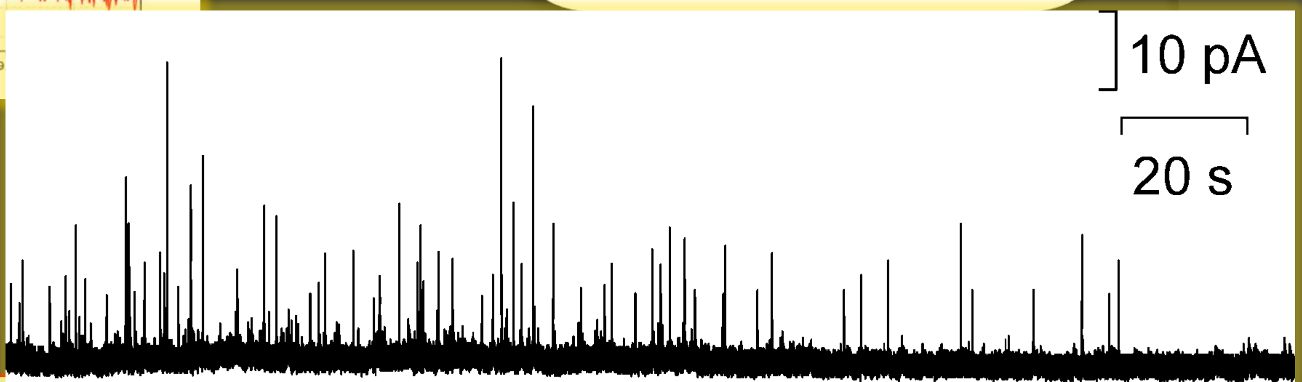

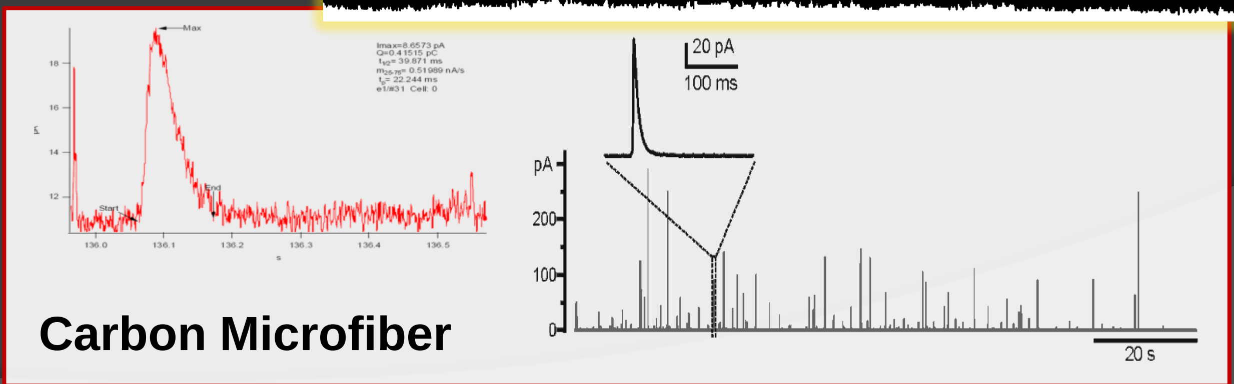

Conclusions

- ✓ **Fabrication of graphite-like conductive channels ($\rho \sim 10^{-3}\ \Omega\cdot cm$) buried in a transparent and highly insulating ($\rho > 10^{14}\ \Omega\cdot cm$) diamond matrix**
  - ⇒ exclusive ion beam process (not additional contacting methods required)
  - ⇒ application of a novel method based on metal variable thickness masks to modulate the channels depth
- ✓ Channels electrical characterization
  - ⇒ Variable Range Hopping on as-implanted/low fluence implantation channels
  - ⇒ graphitization on annealed sample
- ✓ **First prototype of biosensors was realized**
  - ⇒ measurement of exocytose was performed

future activities…

Near future activities…

- diamond:
  - CVD,
  - single crystal,
  - type IIa,
  - 4.5×4.5×1.5 mm^3
- He @ 1.8 MeV
- thermal annealing @ 1100 °C ×2 hours

9 channels

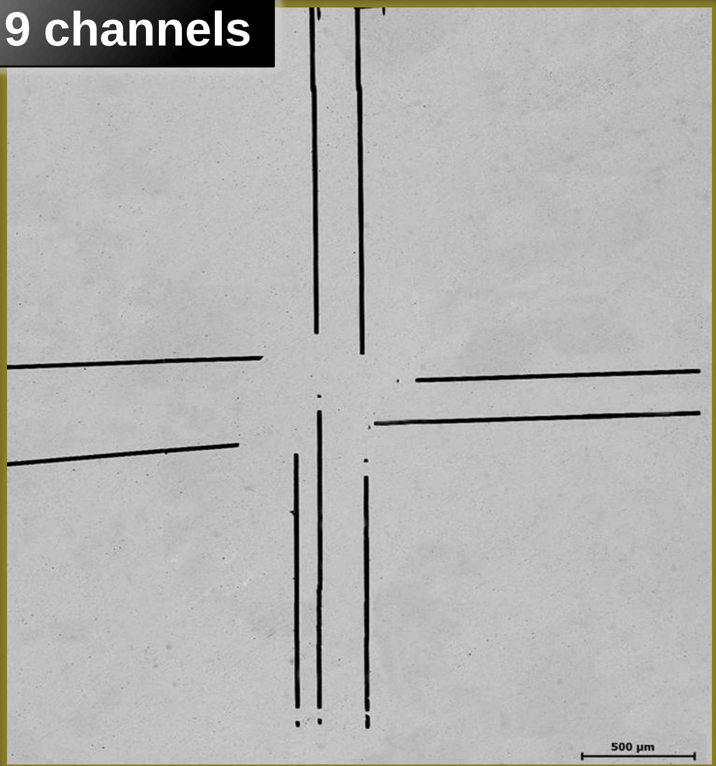

MULTI ELECTRODES ARRAY FOR EXOCYTOSES DETECTION OF CELL CULTURE

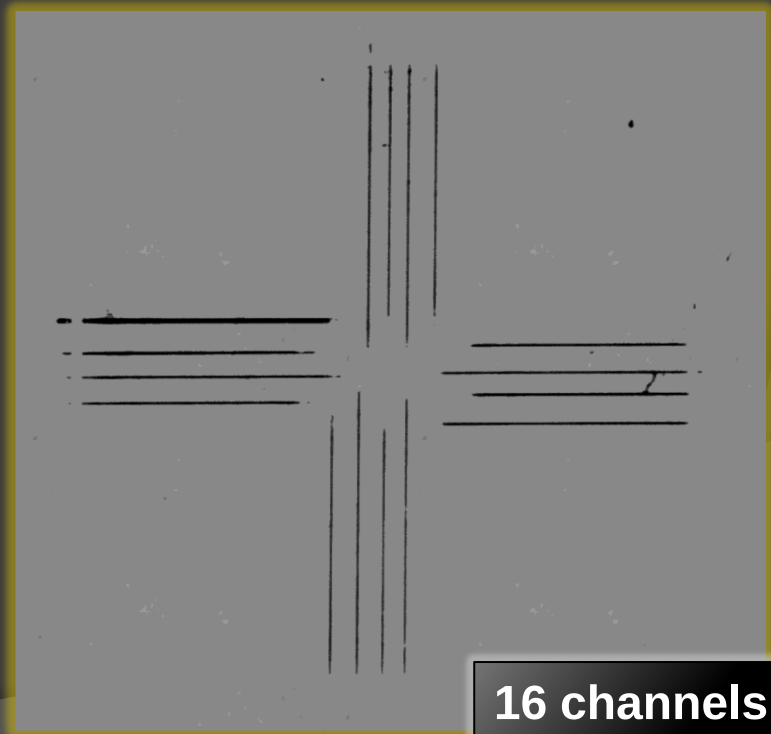

16 channels

Near future activities…

MULTIPLE POINTS EXOCYTOSE DETECTION FROM A SINGLE CELL

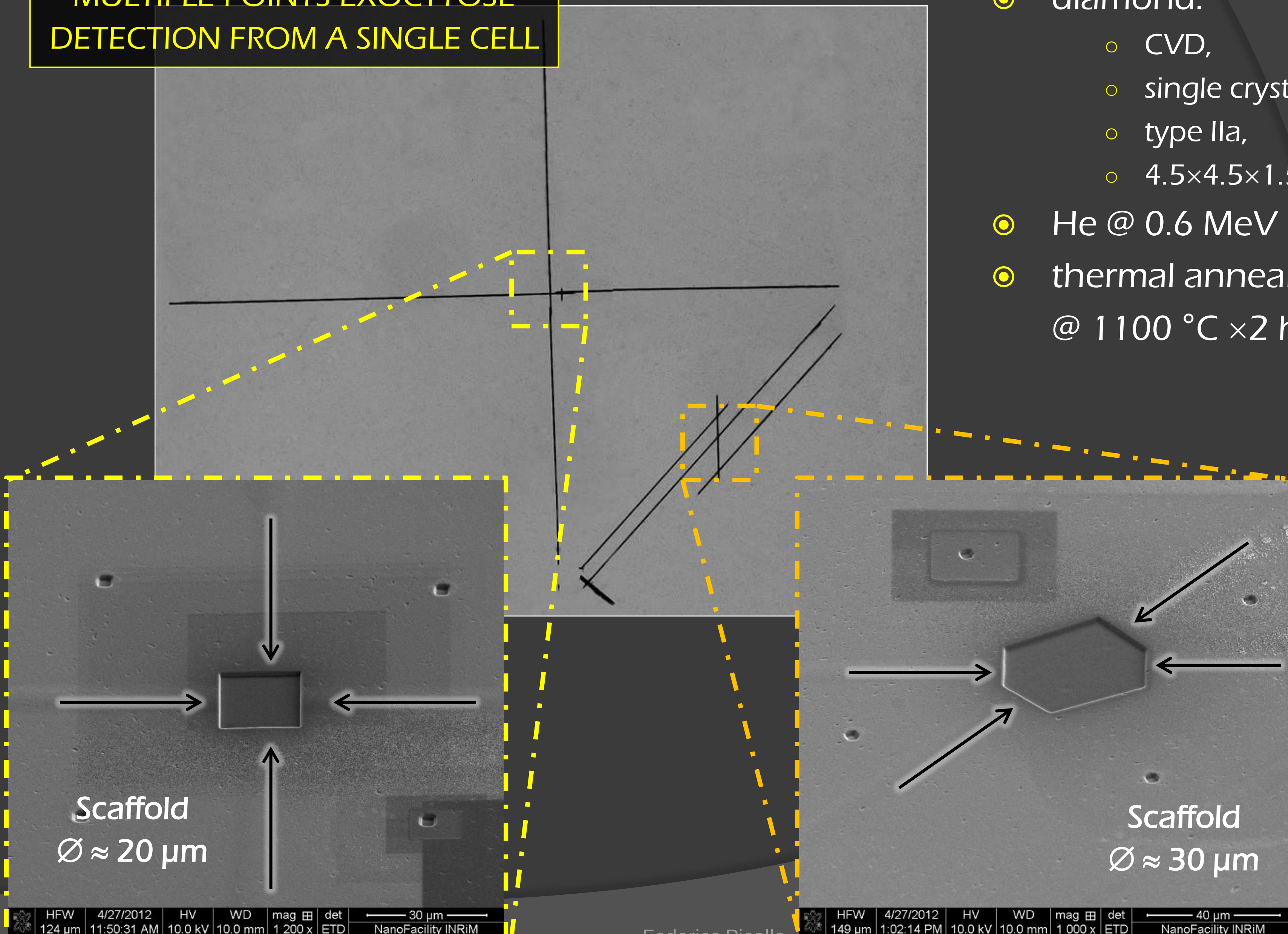

- diamond:
  - CVD,
  - single crystal,
  - type IIa,
  - 4.5×4.5×1.5 mm^3
- He @ 0.6 MeV
- thermal annealing @ 1100 °C ×2 hours

Acknowledgements

Sample processing and characterization
→ University of Torino
P. Olivero, D. Gatto Monticone, S. Gosso, V. Carabelli, A. Lo Giudice, E. Carbone, E. Vittone

FIB micromachining
→ National Institute of Metrologic Research
G. Amato, L. Boarino, E. Enrico

MeV ion implantation
→ Ruđer Bošković Institute
M. Jakšić, Ž. Pastuović, N. Skukan

→ National Laboratories of Legnaro (INFN)
V. Rigato, L. La Torre, G. Legnaro

MeV ion implantation, FIB microfabrication and cross-sectional TEM
→ MARC group, University of Melbourne
B. Fairchild , S. Prawer, S. Rubanov

Signal conditioning electronics
→ Institute of Electron Devices and Circuits, Ulm University, Germany
A. Pasquarelli

Thank you for your attention!!